Zhou *et al.*
*European Journal of Medical Research* (2025) 30:43
https://doi.org/10.1186/s40001-024-02186-8

European Journal of Medical Research

RESEARCH Open Access

# MVK, induced by Kras, represses cGAS-Sting signalling in lung adenocarcinoma

Changsheng Zhou[1†], Jia Liu[2†], Xudong Hu[3†], Lu Lu[1], Juan Hou[4], Jian Wang[1], Liqun Jiang[5], Shuangshuang Huang[1], Yu Lin[6], Luyao Liu[7], Lingling Cui[8*], Yiqian Liu[7*] and Yufeng Huang[4*]

## Abstract

Cholesterol metabolism is abnormally active in tumour cells. Metabolic enzymes related to cholesterol metabolism are upregulated in tumours, but their nonmetabolic functions remain unclear. We found that MVK (mevalonate kinase) is upregulated in lung adenocarcinoma tissues vs. normal tissues and that its expression can be induced by constitutively activated Kras. By investigating the molecular mechanisms involved, we discovered that MVK interacts with TBK1, inhibiting TBK1 phosphorylation and thereby suppressing cGAS-Sting signalling. In addition, we found a negative correlation between MVK expression and $CD8^+$ T-cell infiltration via a public database analysis. In summary, our study demonstrates the importance of the nonmetabolic function of MVK in modifying the immunological milieu and provides new targets for lung adenocarcinoma therapy.

**Keywords** Mevalonate kinase, Lung adenocarcinoma, CGAS-Sting signalling, Kras

## Introduction

One key feature differentiating tumour cells from normal cells is metabolic reprogramming [1]. During the progression of various tumours, abnormal cholesterol synthesis metabolism is very common [2]. High serum levels of cholesterol increase the antitumour functions of natural killer cells, and the accumulation of cholesterol in macrophages and other immune cells promotes inflammatory responses. However, the functions of enzymes involved in cholesterol metabolism (especially nonmetabolic functions) in tumour progression have not been fully elucidated.

Mevalonate kinase (MVK) is a key enzyme in cholesterol metabolism and is responsible for the phosphorylation of the metabolic intermediate mevalonate [3]. Studies have indicated that many metabolic enzymes (such as NME7 and PKM2) perform nonmetabolic functions [4, 5]. The nonmetabolic functions of these enzymes include the promotion of tumour cell growth, invasion, and metastasis [4, 5]. However, it is currently unclear whether MVK has nonmetabolic functions.

†Changsheng Zhou, Jia Liu and Xudong Hu have contributed equally to this work.

*Correspondence:
Lingling Cui
cll@zzu.edu.cn
Yiqian Liu
liuyiqian@njmu.edu.cn
Yufeng Huang
one1210@126.com
[1] Departments of Respiratory and Critical Care Medicine, The Affiliated Cangnan Hospital of Wenzhou Medical University, Cangnan, Zhejiang 325800, China
[2] Department of Clinical Laboratory, Jingjiang People's Hospital Affiliated With Yangzhou University, Jingjiang 214500, China
[3] Shanghai Institute of Thoracic Oncology, Shanghai Chest Hospital, Shanghai Jiao Tong University School of Medicine, Shanghai 200030, China
[4] Department of Oncology, Jingjiang People's Hospital Affiliated With Yangzhou University, Jingjiang 214500, China
[5] Department of Thoracic Surgery, Jingjiang People's Hospital Affiliated With Yangzhou University, Jingjiang 214500, China
[6] Department of Oncology, the Affiliated Suzhou Hospital of Nanjing Medical University, Suzhou 215001, Jiangsu, China
[7] Department of Oncology, The First Affiliated Hospital of Nanjing Medical University, Nanjing 210029, China
[8] College of Public Health, Zhengzhou University, Zhengzhou 450001, China

The cGAS-Sting signalling pathway is widely involved in physiological and pathological processes [6, 7]. The stimulator of interferon genes (STING) pathway is an essential regulator of innate immunity and a key DNA-sensing process [7, 8]. Sting is located within the endoplasmic reticulum and comprises four transmembrane helices and a spherical C-terminal domain that protrudes into the cytoplasm [8]. As an intracellular receptor for cGAMP, Sting closes its ligand-binding pocket upon binding with cGAMP and releases its C-terminus, recruiting TBK1 and IRF3, thereby upregulating the expression of downstream IFNα and IFNβ [9]. cGAS-Sting signalling pathway activation increases immunotherapy efficacy by facilitating immune cell infiltration into tumour tissues [8]. Phosphorylation of serine 172 in TBK1 is a hallmark of its activation [8, 9]. However, the regulatory mechanisms of its activity are poorly understood.

This study aimed to explore the MVK expression pattern in non-small cell lung cancer as well as the underlying molecular mechanisms.

## Materials and methods

### Cell culture

Lung adenocarcinoma cell lines (H1299, A549, H23, PC-9, H1793, H1437, H441, H2030, and H1792) and normal bronchial epithelial (HBE) cells were obtained from the Chinese Academy of Sciences Cell Bank. All human cell lines were authenticated using STR (or SNP) profiling. In addition to antibiotics (100 g/mL streptomycin and 100 U/mL penicillin), 10% fetal bovine serum was added to the DMEM. Every cell line was maintained at 37 °C in an incubator in a 5% $CO_2$ environment. Lipofectamine 8000 was used to transfect cells following the instructions provided by the manufacturer.

### Clinical samples

We obtained cancerous tissues and adjacent noncancerous tissues from Jingjiang People's Hospital. Patient informed consent was obtained before any tissue samples were collected to study MVK expression levels. The Ethics Committee of Jingjiang People's Hospital approved all relevant experiments in this study (2024-KY-002–08).

### Western blotting

Inhibitors of phosphatase and protease were added to RIPA lysis buffer. For the cell culture, the cells were washed twice with PBS before lysis buffer was added. After being frozen in liquid nitrogen, the tissues were crushed and treated with an ice-based RIPA lysis solution. After the cell lysate was centrifuged and the supernatant was collected, the protein concentration was measured using a BCA protein assay kit. Using SDS–PAGE, equal amounts of proteins were separated and transferred to a PVDF membrane. Following overnight incubation at 4 °C with primary antibodies, the membrane was incubated with secondary antibodies conjugated with HRP for 1–2 h. The immunosignals were detected using a chemiluminescent reagent (Millipore, WBKLS0050). The analysis was conducted via Image Lab software. Primary antibodies were utilized in this study: MVK (ProteinTech, 12,228–1-AP, 1:1000), tubulin (Santa Cruz Biotechnology, sc-5286, 1:4000), Flag (ProteinTech, 66,008–4-Ig, 1:1000), TBK1 (ProteinTech, 28,397–1-AP, 1:1000), p-TBK1 (Abcam, ab186469, 1:1000), GST tag (Abcam, ab307273, 1:1000), HA (ProteinTech, 66,006–2-Ig, 1:1000), and GAPDH (ProteinTech, 10,494–1-AP, 1:1000).

### Multiplex immunofluorescence staining

After slicing, dewaxing and antigen retrieval, the endogenous peroxidase was blocked with 3% $H_2O_2$ and washed with running water. 10% goat serum was used for blocking nonspecific binding. The sections were incubated with the primary antibody overnight, washed 3 times with TBST after rewarming. Then, the sections were incubated with goat anti-rabbit IgG H&L (HRP) secondary antibody at room temperature for 1 h, followed by TSA staining and elution. The primary antibody and the secondary antibody of another molecule are incubated again. The sections were stained and sealed for microscopic examination.

### Immunohistochemistry

The tissue sections were dewaxed, rehydrated, and immersed in EDTA for 30 min to improve high-temperature antigen retrieval. An endogenous peroxidase blocking agent was used to block endogenous peroxidase activity for 15 min after the temperature was decreased to room temperature. After that, the samples were washed with PBS 1–2 times. The tissue sections were incubated at 4 °C overnight with MVK antibody (Sigma, HPA016961, 1:200). The tissue sections were subsequently incubated with the secondary antibody for two hours at room temperature. Then, PBS was used to wash the tissue sections three times. Finally, the immunohistochemical reaction was observed using 3,3'-diaminobenzidine (DAB). After every tissue section was counterstained with hematoxylin, the Vectra2 system automatically rated the staining intensity and protein expression levels.

### qPCR

The Takara PrimeScript™ RT Reagent Kit was used to synthesize cDNA from 1 μg of RNA according to the manufacturer's instructions. The extraction of RNA was performed using TRIzol (Invitrogen). The CFX96

real-time fluorescence quantitative PCR detection equipment (Bio-Rad, Richmond, CA, USA) and the SYBR Green kit were used for the qPCR analysis. For the qPCR analysis, actin served as the internal control. The $2^{-\Delta\Delta Ct}$ method was used to determine the expression of the target genes. The primer sequences for actin were as follows: forward primer, 5'-CATGTACGTTGCTATCCA GGC-3', and reverse primer, 5'-CTCCTTAATGTCACG CACGAT-3'. The primer sequences for IFNα were as follows: forward primer, 5'-GCCTCGCCCTTTGCTTTA CT-3'; reverse primer, 5'-CTGTGGGTCTCAGGGAGA TCA-3'. The primer sequences for IFNβ were as follows: forward primer, 5'-ATGACCAACAAGTGTCTCCTCC-3'; reverse primer, 5'-GGAATCCAAGCAAGTTGT AGCTC-3'.

#### Coimmunoprecipitation

Protease and phosphatase inhibitors were added to the IP lysis buffer after the cells were treated to lyse the cells, and interactions between endogenously expressed proteins were examined. After the samples were centrifuged to collect the supernatant, 1 μg of antibody was added, and the mixture was incubated at 4 °C overnight. The following day, 40 μL of protein A/G beads (Bimake, B2302) were added to the mixture, which was then incubated at 4 °C for 4 h. Following three washes with wash buffer, loading buffer (1×) was added to the beads for Western blot analysis.

#### GST pull-down

Glutathione Sepharose 4B beads (GE Healthcare) were washed with a wash solution consisting of 50 mM Tris–HCl (pH 8.0), 150 mM NaCl, and 1% NP-40. The mixture of cell lysates and 10 μg of GST-MVK fusion protein was incubated at 4 °C overnight, after which the mixture was incubated with the beads for an extra 4 h. The beads were subsequently washed with wash solution containing 50 mM Tris–HCl (pH 8.0), 1% NP-40, and 1 mM NaCl three times before 1 × loading buffer was added and heated to 100 °C for 5 min. We collected the supernatant for Western blot analysis.

#### Soft agar assay

When the cell confluence reached approximately 70%, the cells were digested, and the cell suspensions were prepared. First, 1 ml of PBS buffer was added to each well of the 24-well plates, and the PBS buffer in the middle 8 wells was then discarded. Base agar (20% FBS, 40% 2 × DMEM, 40% 1.25% agar) was prepared. 400 μl of base agar was added to each well of a 24-well plate. The top agar (25% FBS, 37.5% 2 × DMEM, 37.5% 1% agar, 2 mM L-glutamine) was then prepared and mixed with the cell suspension ($1 \times 10^3$ cells per well). After the base agar solidified, 400 μl of the top agar was added to each well of the 24-well plates and incubated (5% $CO_2$, 37 °C) for 10–14 days. Four randomly selected fields of view were photographed, and cell colonies were counted under a microscope.

#### Tumorigenesis assay in the mice and ethics statement

The animal procedures were authorized by the ethics committee of Nanjing medical University. Male C57 mice aged 6 weeks were utilized, and $2 \times 10^6$ MVK-knockdown cells or control cells were injected under the skin. Tumors were harvested 3 weeks later. The infiltration of $CD3^+$ T cells and $CD8^+$ T cells were examined using immunofluorescence staining using antibodies against CD3 and CD8.

#### Statistical analysis

The means ± SDs were used to express the experimental results. The data were analyzed via *t* tests. We analyzed the data via the log-rank test and generated survival curves via the Kaplan–Meier method. The statistical analyses were performed with SPSS 17.0 and GraphPad Prism 8 software.

## Results

#### Upregulation of MVK expression in lung adenocarcinoma

The Kaplan–Meier database was used to perform initial studies on the relationship between MVK expression and survival in non-small cell lung cancer patients. The results revealed a strong correlation between elevated MVK expression and poor prognosis in lung adenocarcinoma patients but not in lung squamous cell carcinoma patients (Fig. 1A). Compared with that in normal human bronchial epithelial (HBE) cells, MVK expression was upregulated in lung adenocarcinoma cell lines (Fig. 1B). Furthermore, Western blot analyses revealed that lung adenocarcinoma tissues presented higher levels of MVK expression than paired adjacent tissues did (Fig. 1C). These experimental results were further validated via immunohistochemistry (Fig. 1D, E). Together, these findings indicate that MVK is likely essential in the progression of lung adenocarcinomas.

#### Constitutive activation of Kras induces MVK expression

The Kras gene is mutated and constitutively activated in lung adenocarcinoma [10]. Next, we investigated the effect of constitutively active Kras on MVK protein levels. We first overexpressed constitutively active Kras ($Kras^{G12C}$) in H1299 and H1793 cells (these two cell lines harbour wild-type Kras) and assessed MVK expression. The findings revealed that overexpression of $Kras^{G12C}$ increased the protein level of MVK (Fig. 2A). Compared with that in lung adenocarcinoma cells harbouring wild-type Kras, lung adenocarcinoma cells harbouring

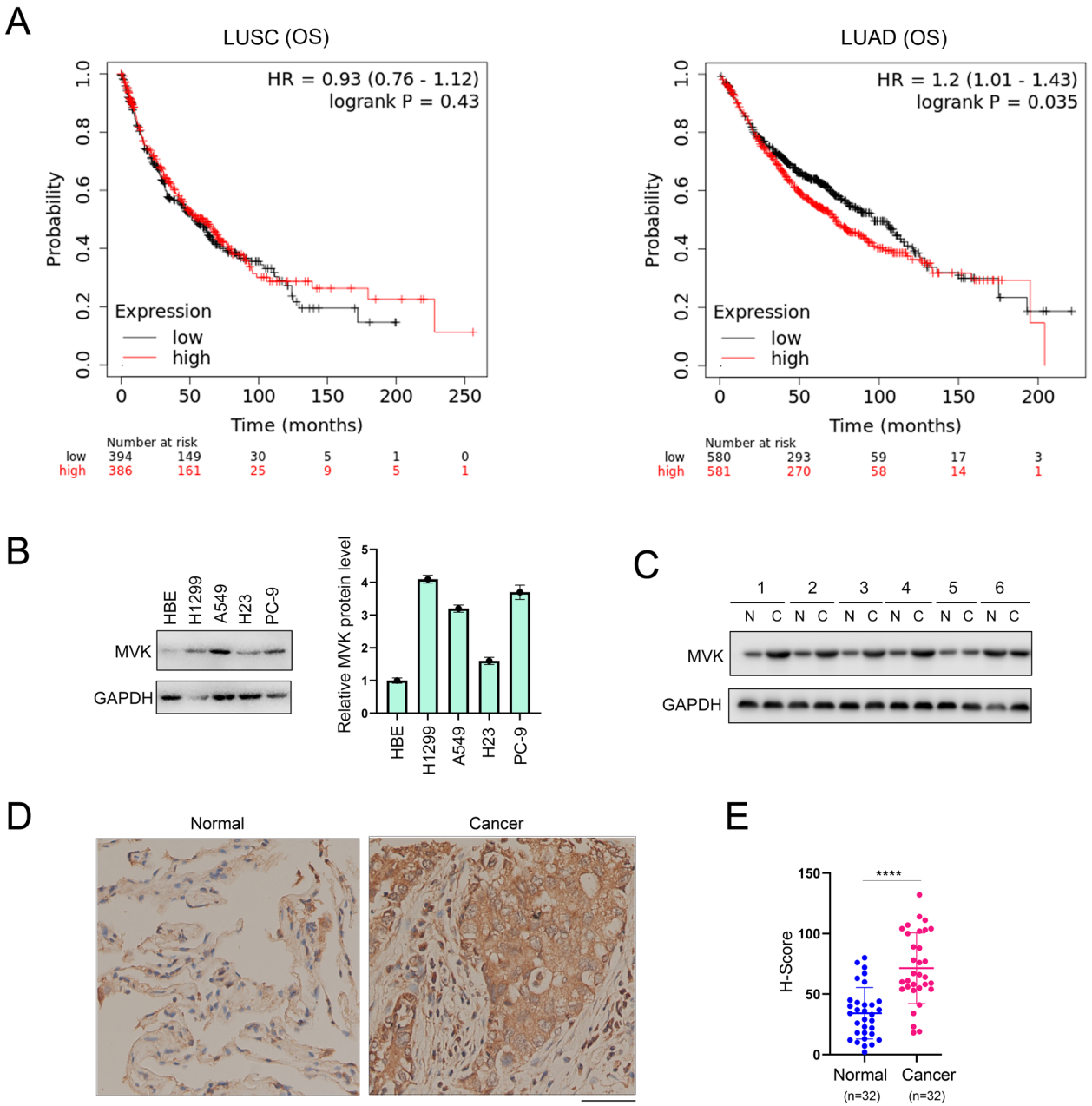


**Fig. 1** Upregulation of MVK expression in lung adenocarcinoma. **A** Comparison of MVK expression and survival between patients with lung adenocarcinoma and patients with lung squamous cell carcinoma via the Kaplan–Meier method. **B** Western blot analysis was used to determine MVK protein levels in lung adenocarcinoma cell lines and normal bronchial epithelial (HBE) cells. Grayscale analysis was performed. **C** Western blot analysis was used to assess the amount of MVK protein in lung adenocarcinoma samples and adjacent normal tissues. **D**–**E** MVK protein levels in lung adenocarcinoma samples and adjacent normal tissues were determined via immunohistochemical staining and statistical analysis. ****, $P < 0.0001$

(See figure on next page.)

**Fig. 2** Constitutive activation of Kras (Kras$^{G12C}$) upregulates MVK expression. **A** Kras$^{G12C}$ overexpression in H1299 and H1793 cells and its ability to induce MVK protein expression were assessed via Western blotting. (**B**) Detection of MVK protein levels in lung adenocarcinoma cells harbouring wild-type Kras or mutant Kras via Western blotting. **C** Detection of MVK protein levels in lung adenocarcinoma tissues harbouring wild-type Kras or mutant Kras via Western blotting. **D**–**E** Assessment of the effect of MVK knockdown on the malignant phenotype induced by Kras$^{G12C}$ via a soft agar colony formation test and statistical analysis. **, $P < 0.01$; ##, $P < 0.01$

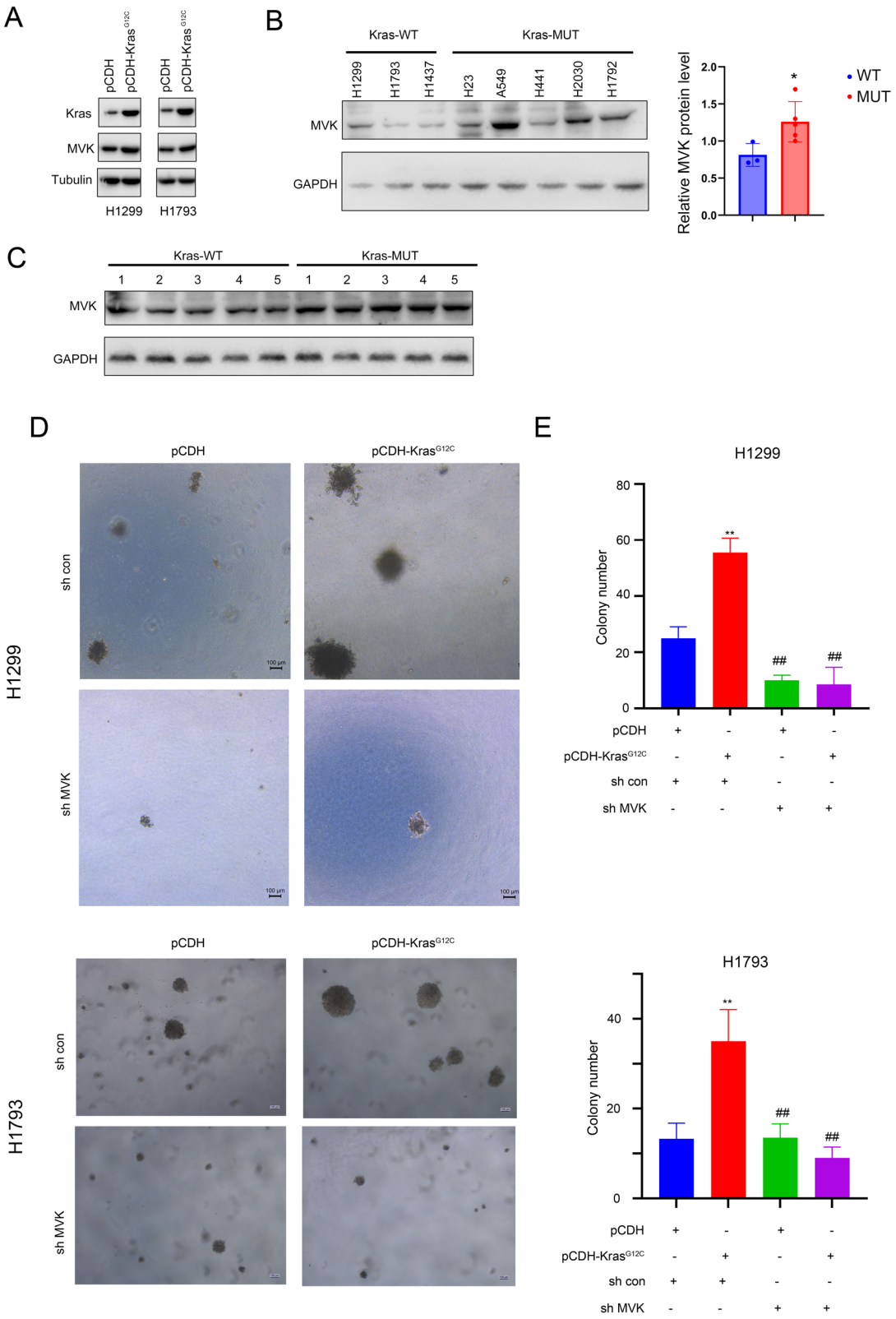


**Fig. 2** (See legend on previous page.)

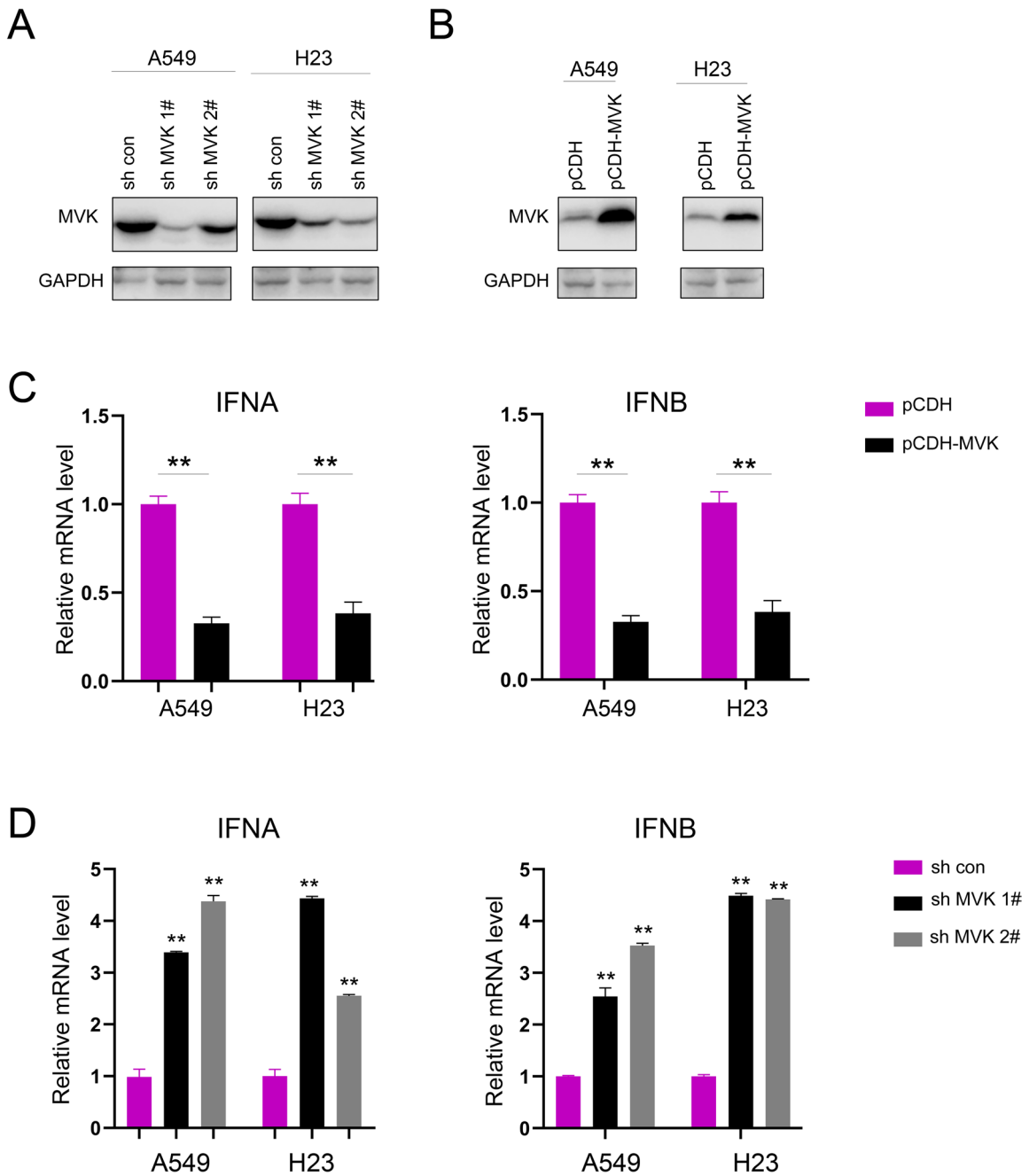


**Fig. 3** MVK inhibits the expression of IFNα and IFNβ. **A** Western blot analysis validated the knockdown of MVK expression in A549 and H23 cells. **B** Western blot analysis validated MVK overexpression in A549 and H23 cells. **C** The effect of MVK overexpression on IFN mRNA levels was assessed via qPCR. **D** qPCR was used to assess the effects of MVK knockdown on IFN mRNA levels. **, $P < 0.01$

constitutively active Kras had greater MVK expression (Fig. 2B). Similarly, lung adenocarcinoma tissues expressing constitutively active Kras had higher levels of MVK expression than did lung adenocarcinoma tissues harbouring wild-type Kras (Fig. 2C). Furthermore, overexpression of $Kras^{G12C}$ in H1299 and H1793 cells promoted anchorage-independent growth, whereas knockdown of MVK expression reversed the malignant phenotype induced by $Kras^{G12C}$ overexpression (Fig. 2D, E). These findings indicate that constitutive activation of Kras induces MVK expression and that MVK expression is essential for the functional effects of constitutively active Kras.

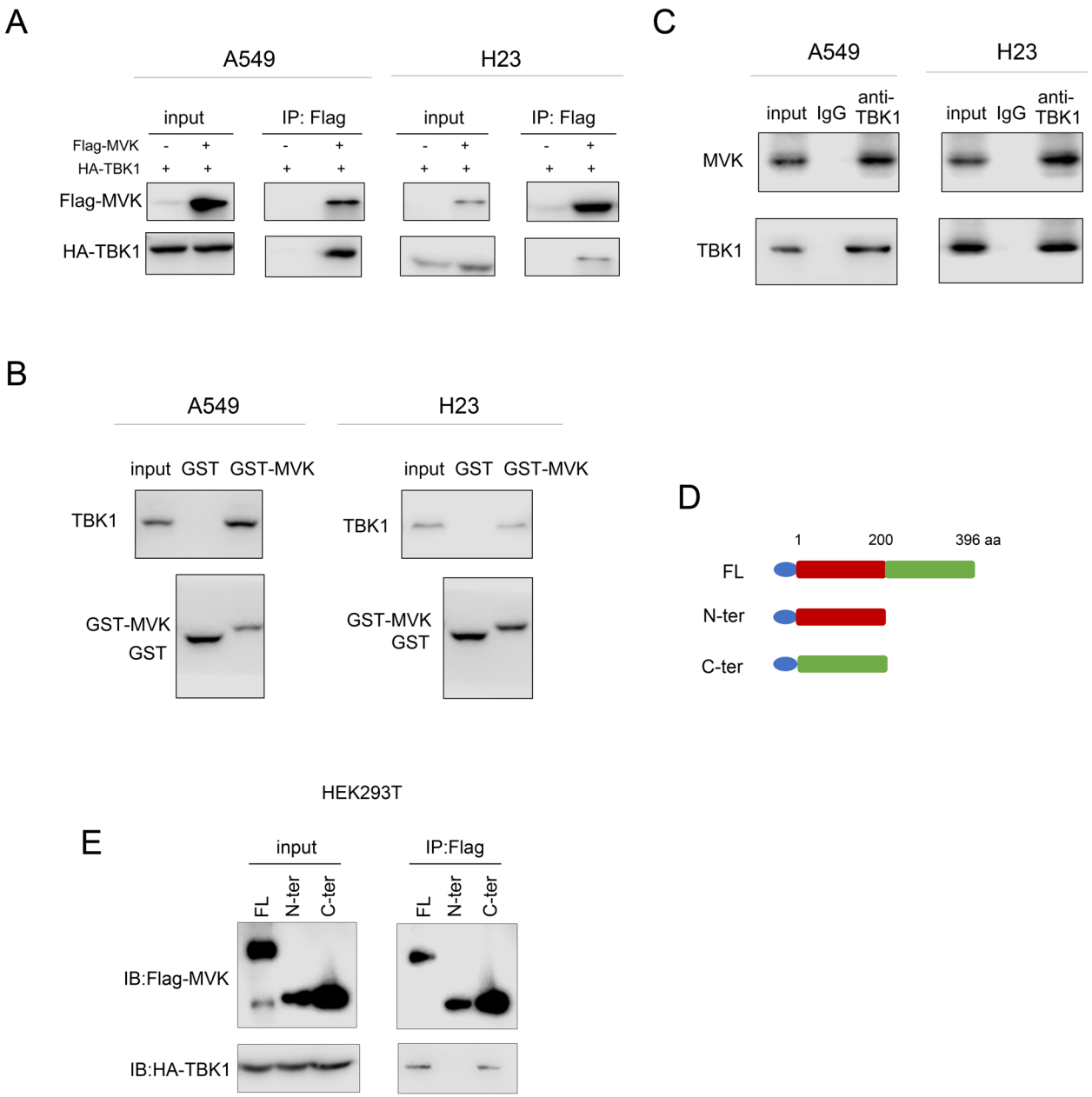


**Fig. 4** Interaction between MVK and TBK1. **A** Coimmunoprecipitation was used to identify the interaction between exogenously expressed TBK1 (HA-TBK1) and MVK (Flag-MVK) in A549 and H23 cells. **B** The interaction between the GST-MVK fusion protein and endogenous TBK1 in A549 and H23 cells was investigated via a GST pull-down assay. **C** Coimmunoprecipitation was performed to investigate the interaction between MVK and TBK1, which is expressed endogenously in A549 and H23 cells. **D** Schematic design of the generated MVK deletion mutant. **E** Coimmunoprecipitation was used to identify the interaction between exogenously expressed TBK1 and the MVK deletion mutant in HEK293T cells

**MVK inhibits the cGAS-Sting signalling pathway**

A key factor in the progression of lung cancer is the cGAS-Sting signalling pathway, which also mediates innate immunity [11, 12]. Next, we investigated how MVK expression affects the cGAS-Sting signalling pathway. We overexpressed MVK in A549 and H23 cells or inhibited MVK expression (Fig. 3A, B). IFNα and IFNβ mRNA levels were decreased upon MVK overexpression, but IFNα and IFNβ expression was promoted when MVK was knocked down (Fig. 3C–D). These findings suggest the mechanism by which MVK regulates the cGAS–Sting signalling pathway.

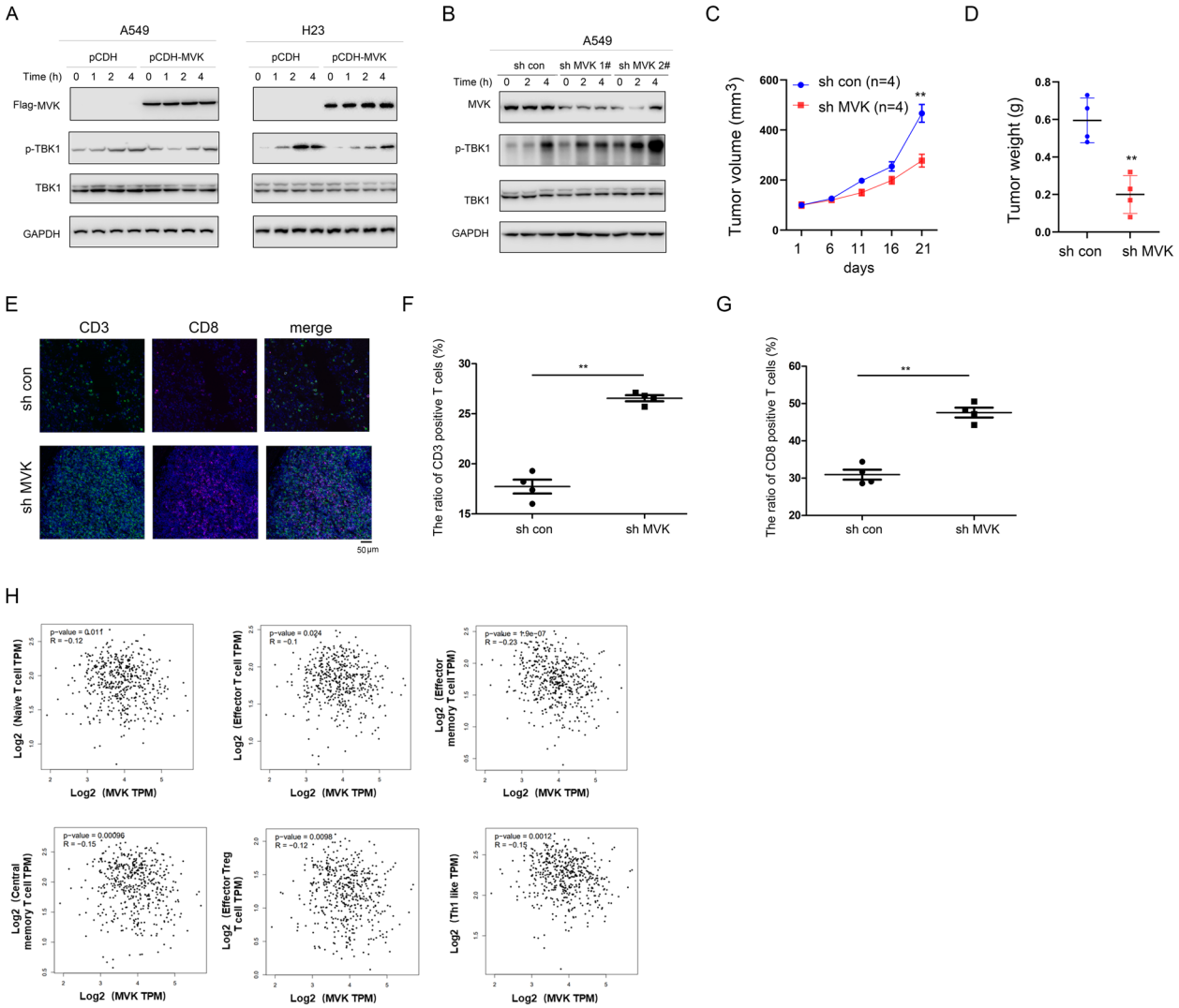


**Fig. 5** MVK negatively regulates TBK1 phosphorylation. **A** Western blot analysis of the effect of MVK overexpression on TBK1 phosphorylation after HT-DNA transfection. **B** Western blotting was used to determine how MVK knockdown affects TBK1 phosphorylation after HT-DNA transfection. **C**–**D** Tumour growth curve and tumour weights were shown. **E**–**G** Immunofluorescence staining was used to assess the infiltration of $CD3^+$ and $CD8^+$ T cells in lung cancer tissues, along with statistical analysis. **H** The correlation between MVK expression and T-cell infiltration was analysed in lung cancer tissues from a public database. **, $P < 0.01$

### Interaction between MVK and TBK1

To elucidate the molecular mechanism by which MVK regulates the signalling pathway and to determine how MVK interacts with crucial elements of the cGAS-Sting signalling pathway, we performed coimmunoprecipitation experiments. The results revealed that TBK1 (HA-TBK1) interacted with exogenously expressed MVK (Flag-MVK) (Fig. 4A). In the GST pull-down experiments, endogenously expressed TBK1 bound to the GST-MVK fusion protein (Fig. 4B). More importantly, endogenously expressed TBK1 in A549 and H23 cells formed a complex with MVK (Fig. 4C). Next, we mapped the domain of the MVK protein that interacts with TBK1 and found that the C-terminus of MVK interacts with TBK1 (Fig. 4D, E).

### MVK inhibits the phosphorylation of TBK1

The effect of MVK expression on TBK1 phosphorylation was then investigated. MVK overexpression inhibited the phosphorylation of TBK1 at the 172nd residue upon HT-DNA transfection (Fig. 5A), whereas knocking down MVK expression promoted its phosphorylation at the same residue (Fig. 5B). We inhibited MVK

expression in LLC cells and performed in situ lung injections. Knocking down MVK impaired the tumorigenicity of LLC cells, which was confirmed by the impairment of tumour growth (Fig. 5C) and decrease in tumour weight (Fig. 5D). Then, we assessed $CD8^+$ T-cell infiltration in the resulting tumours. According to the experimental findings, an increase in $CD8^+$ T-cell infiltration following MVK expression knockdown was observed (Fig. 5E–G). Moreover, MVK expression was inversely correlated with T-cell infiltration in lung cancer tissues in a public database analysis (Fig. 5H). Therefore, the regulatory role of MVK in the immune milieu of tumours is further supported by these findings.

## Discussion

The nonmetabolic functions of metabolic enzymes in tumour metabolism have been a research hotspot. For example, PKM2 influences global gene transcription by phosphorylating histone 3 through its protein kinase function [5]. Additionally, PKM2 can phosphorylate Bub3, leading to chromosome aggregation and promotion of cell mitosis [13]. The role of abnormal cholesterol metabolism in tumour progression has gradually been recognized [14]; however, it remains unclear whether enzymes involved in cholesterol metabolism have nonmetabolic functions. In the present study, we found that MVK inhibits the phosphorylation of TBK1, which inhibits the cGAS-Sting signalling pathway.

The level of MVK expression in lung squamous cell carcinoma is equivalent to that in adjacent normal tissues. On the other hand, compared with adjacent normal tissues, lung adenocarcinoma tissues presented elevated MVK expression. This expression pattern of MVK suggests its significant role in the progression of lung adenocarcinoma. In this study, constitutively activated Kras induced the expression of MVK, and Kras mutations are very common in adenocarcinoma. This finding also explains why MVK is upregulated in adenocarcinoma. Small molecules that target constitutively activated Kras are still in clinical trials [15]. For non-small cell lung cancer harbouring active Kras mutations, targeting MVK might be an effective treatment.

The inhibitory effect of MVK on TBK1 phosphorylation is another important finding from this study. When cGAMP binds to Sting, the C-terminal conformation of cGAMP changes to recruit TBK1 and IRF3. There have been several studies on the regulation of TBK1 activity. For example, GSK3β can phosphorylate TBK1, activating its kinase activity [16]. However, the regulatory role of metabolic enzymes in TBK1 activity and tumour metabolism remains unknown. This study reveals the inhibitory effect of MVK, a key enzyme in cholesterol metabolism, on TBK1 activity, providing new insights into the regulation of TBK1 kinase activity.

## Conclusion

Taken together, the results of this study revealed that MVK is upregulated in lung adenocarcinoma and likely promotes its progression by inhibiting the cGAS-Sting pathway.

### Abbreviations

MVK Mevalonate kinase
STING The stimulator of interferon genes

### Author contributions

HYF, LYQ, and CLL designed this study and drafted the manuscript. ZCS, LJ and HXD helped collect the data and performed statistical analysis. LL, HJ, WJ, JLQ, HSS, LY and LLY contributed to the conception, design, data interpretation, and supervision of the study. All the authors read and approved the manuscript.

### Funding

Not applicable.

### Availability of data and materials

No datasets were generated or analysed during the current study.

## Declarations

### Ethics approval and consent to participate

The animal procedures were authorized by the ethics committee of Nanjing medical University (E24-17), and were compliance with all relevant ethical regulations.

### Competing interests

The authors declare no competing interests.

Received: 29 September 2024 Accepted: 30 November 2024
Published online: 22 January 2025

### References

1. Stine ZE, Schug ZT, Salvino JM, Dang CV. Targeting cancer metabolism in the era of precision oncology. Nat Rev Drug Discov. 2022;21(2):141–62.
2. Zeng Y, Luo Y, Zhao K, Liu S, Wu K, Wu Y, Du K, Pan W, Dai Y, Liu Y, Ren M, Tian F, Zhou L, Gu C. m6A-mediated induction of 7-dehydrocholesterol reductase stimulates cholesterol synthesis and cAMP signaling to promote bladder cancer metastasis. Can Res. 2024;84(20):3402–18.
3. Chen Z, Zhou X, Zhou X, Tang Y, Lu M, Zhao J, Tian C, Wu M, Liu Y, Prochownik EV, Wang F, Li Y. Phosphomevalonate kinase controls β-catenin signaling via the metabolite 5-diphosphomevalonate. Adv sci. 2023. https://doi.org/10.1002/advs.202204909.
4. Ren X, Rong Z, Liu X, Gao J, Xu X, Zi Y, Mu Y, Guan Y, Cao Z, Zhang Y, Zeng Z, Fan Q, Wang X, Pei Q, Wang X, Xin H, Li Z, Nie Y, Qiu Z, Li N, Sun L, Deng Y. The protein kinase activity of NME7 activates Wnt/β-catenin signaling to promote one-carbon metabolism in hepatocellular carcinoma. Can Res. 2022;82(1):60–74.
5. Yang W, Xia Y, Hawke D, Li X, Liang J, Xing D, Aldape K, Hunter T, Alfred Yung WK, Lu Z. PKM2 phosphorylates histone H3 and promotes gene transcription and tumorigenesis. Cell. 2012. https://doi.org/10.1016/j.cell.2012.07.018.
6. Minton K. Lipid metabolism extinguishes cGAS-STING-induced inflammation. Nat Rev Immunol. 2023;23(12):785.

7. Hornung V, Hartmann R, Ablasser A, Hopfner KP. OAS proteins and cGAS: unifying concepts in sensing and responding to cytosolic nucleic acids. Nat Rev Immunol. 2014;14(8):521–8.
8. Hopfner KP, Hornung V. Molecular mechanisms and cellular functions of cGAS-STING signalling. Nat Rev Mol Cell Biol. 2020;21(9):501–21.
9. Motwani M, Pesiridis S, Fitzgerald KA. DNA sensing by the cGAS-STING pathway in health and disease. Nat Rev Genet. 2019;20(11):657–74.
10. Reck M, Carbone DP, Garassino M, Barlesi F. Targeting KRAS in non-small-cell lung cancer: recent progress and new approaches. Annal Oncol. 2021;32(9):1101–10.
11. Zierhut C, Yamaguchi N, Paredes M, Luo JD, Carroll T, Funabiki H. The cytoplasmic DNA sensor cGAS promotes mitotic cell death. Cell. 2019;178(2):302-315.e323.
12. Sen T, Rodriguez BL, Chen L, Corte CMD, Morikawa N, Fujimoto J, Cristea S, Nguyen T, Diao L, Li L, Fan Y, Yang Y, Wang J, Glisson BS, Wistuba J II, Sage JV, Heymach DL, Gibbons LAB. Targeting DNA damage response promotes antitumor immunity through STING-mediated T-cell activation in small Cell lung cancer. Cancer Discov. 2019;9(5):646–61.
13. Jiang Y, Li X, Yang W, Hawke DH, Zheng Y, Xia Y, Aldape K, Wei C, Guo F, Chen Y, Lu Z. PKM2 regulates chromosome segregation and mitosis progression of tumor cells. Mol Cell. 2014;53(1):75–87.
14. Huang B, Song BL, Xu C. Cholesterol metabolism in cancer: mechanisms and therapeutic opportunities. Nat Metab. 2020;2(2):132–41.
15. Negri F, Bottarelli L, de'Angelis GL, Gnetti L. KRAS: a druggable target in colon cancer patients. Int J Mol Sci. 2022;23(8):4120.
16. Lei CQ, Zhong B, Zhang Y, Zhang J, Wang S, Shu HB. Glycogen synthase kinase 3β regulates IRF3 transcription factor-mediated antiviral response via activation of the kinase TBK1. Immunity. 2010;33(6):878–89.

## Publisher's Note